BULLETIN OF THE CHEMICAL SOCIETY OF JAPAN VOL. 42 1271—1277 (1969)

Thermodynamic Properties and Phase Transitions of Thallous Cyanide Crystal

Takasuke MATSUO, Masayasu SUGISAKI,*1 Hiroshi SUGA and Syûzô SEKI

Department of Chemistry, Faculty of Science, Osaka University, Toyonaka, Osaka

(Received October 9, 1968)

The heat capacities of TlCN crystal were measured from 15 to 300°K with an adiabatic calorimeter. Three regions of anomalously high heat capacity were discovered. Thermodynamic functions of the crystal were calculated by the graphical integration of the heat capacity data. ^{205}Tl nuclear magnetic resonance was observed as functions of temperature and applied static magnetic field. Their second moment values could be interpreted in terms of the anisotropic chemical shift tensor.

The alkali cyanides, NaCN, KCN, RbCN and CsCN all crystallize in the cubic system at room temperature and on cooling, they all transform into the less symmetric modifications. Their thermodynamic behaviors were reported in the series of our papers.[1-3] The present investigation deals with thallous cyanide crystal. Thallium belongs to the third group in the periodic table but its monovalent ion behaves much like the alkali ions. Thus, its hydroxide is strongly alkaline in aqueous solution and it forms halide crystals of similar structure. Therefore, its cyanide was expected to exhibit some properties analogous to those of the alkali cyanides.

We present here the results of low temperature heat capacity measurement carried out mainly in order to investigate the phase transition effect.

In addition to the thermodynamic method, thallous compounds can be investigated with the nuclear magnetic resonance. ^{203}Tl and ^{205}Tl nuclei involved with the natural abundance ratio; 29.5%: 70.5%, respectively, have nuclear spin 1/2 with experimentally favorable gyromagnetic ratio. Owing to the large number of electrons which Tl^+ ion has, Tl resonance shows some interesting feature which is absent from the usual proton resonance: we can expect to see the chemical shift and/or indirect nuclear spin coupling in solids.[4]

In spite of its simple composition, very little is known about the property of thallous cyanide crystal, though its chemical reactivity was studied rather extensively.[5] The only relevant works that came into our attention are two structural investigations,[5,6] both dealing with the room temperature cell constant of thallous cyanide crystal. Strada[6] showed that the crystal has the cesium chloride structure with $a=3.83$ Å while Penneman and Staritzky[5] gave $a=3.993$ Å, the latter being in good correlation with other alkali halides and

*1 Present address: Department of Physics, Faculty of Science, The University of Tokyo, Hongo, Tokyo.

1) H. Suga, T. Matsuo and S. Seki, This Bulletin, **38**, 1115 (1965).

2) T. Matsuo, H. Suga and S. Seki, *ibid.*, **41**, 583 (1968).

3) M. Sugisaki, T. Matsuo, H. Suga and S. Seki, *ibid.*, **41**, 1747 (1968).

4) N. Bloembergen and T. J. Rowland, *Phys. Rev.*, **97**, 1679 (1955).

5) R. A. Penneman and E. Staritzky, *J. Inorg. Nuclear Chem.*, **6**, 112 (1958).

6) M. Strada, *atti. acad. Lincei*, **19**, 807 (1934).

cyanides. The cesium chloride structure made up of CN^- ions is just the same situation as in the cesium cyanide crystal. That is, there must be some orientational disorder in the ionic configuration of CN^- group, which means there may be phase transitions at lower temperatures. The same line of reasoning resulted in the previous investigations on NaCN, KCN, RbCN and CsCN.

Experimental

The Sample Preparation. The thallous cyanide crystal was prepared according to the reaction

$$TlOH + HCN \rightarrow TlCN + H_2O,$$

in aqueous solution.

Thallous hydroxide was made by oxidation of metallic thallium in water[7] as follows. Metallic thallium of stated 99.9% purity supplied by Nakarai Chemicals Ltd. in a cylindrical form was machined to turnings on a lathe. 75 g of the turnings was put in a pyrex flask, furnished with a polyethylene stirrer, together with 700 cc of water purified by an ion-exchanger. It was then oxidized by bubbling cylinder oxygen gas from which carbon dioxide had been removed with aqueous solution and pellets of potassium hydroxide. No heating of the reaction vessel was employed lest the alkaline solution might react with the glass are at elevated temperatures. After 24 hr of bubbling, undissolved metal was filtered off the solution.

Hydrogen cyanide was prepared in a standard way, *i.e.*, by mixing aqueous solution of KCN with sulfuric acid and trapping the evolving gas in a glass flask chilled with an ice-salt mixture.

About 70 cc of liquid hydrogen cyanide was poured into 700 cc of aqueous solution of thallous hydroxide obtained as above. As soon as the two liquids were mixed, a white crystalline powder precipitated out. The crystal was filtered off the solution and dried in vacuum at 130°C for 4 hr. The X-ray powder photograph of the crystal taken with Cu$K\alpha$ radiation was assignable to CsCl structure with a lattice constant of $a=3.97$Å.*2 This figure may be accurate about to 1%.

The most susceptible impurity was the carbonate ion, on which we tested the sample as follows. Small amount of the sample was dissolved in water. To the solution, $Ba(OH)_2$ aqueous solution was added. If there was sufficient concentration of carbonate ion in the sample, white precipitate of $BaCO_3$ would be formed. In fact no precipitation was observed in the present case. Comparison with an independent test by using K_2CO_3 solutions of known concentration showed that the present TlCN contains less than 0.1 weight per cent of carbonate ion.

Calorimetry. The heat capacities were measured with an adiabatic calorimeter operating from 15 to 300°K. Its detail was reported elsewhere.[8] The weight of sample used for calorimetry was 29.008 g (0.12591 mol). It was packed in a gold calorimeter cell with a small amount of helium gas to facilitate thermal equilibrium.

In a preliminary run, it was found that there are three temperature regions of anomalously high heat capacity. They are around 90, 190 and 260°K. The lowest one supercools easily and causes objectionable thermal effect. In order to prepare the stable lowest temperature phase, the specimen was first cooled down to 65°K and kept at the temperature overnight. Subsequent annealing at 85°K followed by recooling to 58°K produced the stable phase. At 58°K 1st run was initiated.

Temperature step of 1—2°K was usually chosen for one measurement in the normal region. In the transition regions necessarily smaller step was used. After turning off the calorimeter heater, usually 10 min were sufficient for it to attain a thermal equilibrium. But from 79 to 87°K, more than 20 min were needed. Next anomalous region around 190°K remained unnoticed until the data were processed, for it did not cause any anomalous equilibriating behavior. Another anomalous region is around 266°K where the heat capacity becomes drastically large and also the equilibriating times were more than 1 hr. Since the high temperature (cubic) phase was found to be supercooled to 248°K, nearly 20°K below the normal transition temperature, its heat capacities were measured in this metastable region in order to facilitate determination of the "normal heat capacity."

Nuclear Magnetic Resonance. Tl nuclear magnetic resonance experiment was carried out with a Nihon-Denshi electromagnet and a locally designed spectrometer of Pound-Watkins type, followed by a phase sensitive detector and a recorder. The RF coil was housed in a copper cylinder which was suspended in a glass dewar. The specimen in a glass tube was cooled by nitrogen gas which boiled off the liquid at the bottom of the dewar flask. The sample temperature was monitored with a chromel-P constantan thermocouple attached to the specimen glass tube. The ^{205}Tl resonance signal was recorded between the liquid nitrogen and room temperatures at 10.6 MHz. The ^{203}Tl signal was also detected at room temperature but naturally with weaker intensity. On cooling both ^{205}Tl and ^{203}Tl signal broadened considerably and ^{203}Tl signal was scarcely above the noise level. Therefore, only ^{205}Tl resonance was studied in detail. In addition to the temperature dependence, static field dependence of the resonance line was studeid at 8, 10.6, 15 and 17.5 MHz for two fixed temperatures, 210°K and room temperature.

Experimental Results

Heat Capacity. The experimental molar heat capacities are given in Table 1 in the chronological order. They are the ratios of the molar enthalpy

7) F. Bahr, *Z. anorg. Chem.*, **71**, 81 (1911).

*2 Our datum, though not too accurate, favors Penneman and Staritzky's value rather than Strada's. Strada's value is definitely inconsistent when compared with the lattice parameters of alkali halides, and cyanides. Therefore, citations of Strada's value in some books should be corrected. [For instance; R. W. G. Wyckoff, "Crystal Structures" (2nd edition) Vol. 1, Interscience Publishers, New York (1963), p. 104; J. C. Slater, "Quantum theory of molecules and solids" Vol. III, McGraw-Hill, New York (1965), p. 342.]

8) H. Suga and S. Seki, This Bulletin, **38**, 1000 (1965).

TABLE 1. HEAT CAPACITIES OF THALLOUS CYANIDE CRYSTAL IN J/mol °K

T (°K)	$\Delta H/\Delta T$	ΔT (°K)	T (°K)	$\Delta H/\Delta T$	ΔT (°K)
	Series 1		77.46	52.67	1.097
58.75	41.15	2.188	78.55	53.54	1.084
60.74	43.86	1.814	79.63	54.69	1.070
62.51	44.61	1.930	80.69	56.16	1.054
64.52	45.77	1.883	81.74	58.11	1.035
66.38	46.74	1.842	82.76	61.06	1.010
68.40	47.80	2.205	83.75	66.31	0.971
70.58	48.82	2.155	84.70	72.26	0.932
72.71	49.83	2.112	85.63	72.07	0.929
74.81	50.93	2.069	86.57	67.84	0.951
76.86	52.11	2.030	87.53	63.76	0.974
			88.50	63.16	0.974
	Series 2				
93.38	59.03	1.806		Series 5	
95.18	59.20	1.794	95.83	59.05	1.972
			97.89	59.67	1.953
	Series 3		99.83	60.16	1.937
15.10	9.54	2.126	101.76	60.60	1.927
17.02	11.42	1.723	103.67	61.09	1.908
17.89	12.34	1.585	105.51	61.62	1.893
19.41	13.56	1.398	107.65	62.16	2.272
20.99	14.90	1.178	109.91	62.62	2.254
22.41	15.88	1.608	112.16	63.14	2.237
23.99	17.26	1.578	114.38	63.70	2.219
25.74	18.71	1.891	116.60	64.18	2.203
27.56	20.12	1.714	118.79	64.50	2.189
29.49	21.45	2.126	120.97	65.34	2.171
31.51	23.11	1.943	123.14	65.65	2.150
33.39	24.63	1.799	125.30	65.94	2.149
35.14	26.02	1.685	127.44	66.40	2.136
36.87	27.24	1.775	129.57	66.89	2.123
38.83	28.86	2.124	131.68	67.29	2.112
40.89	29.91	2.003	133.79	67.84	2.100
42.84	31.21	1.902	135.89	68.15	2.090
44.70	32.42	1.816	136.89	68.94	2.061
46.48	33.55	1.741	139.09	69.31	2.315
48.19	34.60	1.676	141.40	69.70	2.303
49.91	35.61	1.772	143.70	70.18	2.221
51.66	36.63	1.715	145.98	70.67	2.281
53.47	37.59	1.906	148.26	70.96	2.271
55.35	38.76	1.846	150.53	71.46	2.260
57.17	39.83	1.794	152.78	72.23	2.248
58.95	41.01	1.746	155.03	72.58	2.236
			157.26	73.04	2.226
	Series 4		159.48	73.48	2.216
76.36	51.78	1.111	161.77	73.98	2.352
164.12	74.21	2.345	261.05	86.94	2.046
166.46	75.17	2.328		Series 7	
168.78	75.39	2.321	279.93	68.02	2.394
171.10	75.93	2.310	282.36	68.20	2.384
173.40	76.47	2.299	287.11	67.86	2.476
175.30	77.32	2.279	289.58	67.69	2.471
177.57	77.77	2.270	292.04	67.83	2.463
179.84	78.35	2.259	294.50	67.86	2.457
182.09	79.04	2.248	296.95	67.79	2.452
184.33	79.77	2.237	299.40	67.77	2.447
186.56	80.55	2.225	301.84	67.83	2.443
188.78	81.40	2.212			
190.99	82.04	2.203		Series 8	
193.19	82.26	2.198	259.82	86.76	2.056
195.39	80.29	2.217	261.83	94.20	1.985
197.63	77.76	2.243	263.50	197.84	1.342
199.88	76.43	2.256	264.59	387.51	0.843
202.13	75.97	2.258	265.47	486.88	0.707
204.39	75.83	2.257	266.08	708.63	0.517
206.65	75.92	2.253	266.70	468.61	0.722
208.90	76.10	2.248	267.49	370.15	0.865
211.14	76.38	2.243	268.45	278.21	1.056
213.39	76.68	2.236	269.64	197.96	1.321
215.62	76.98	2.230	271.14	128.71	1.678
			273.05	95.23	1.938
	Series 6		274.96	82.30	2.087
218.25	77.38	2.218	277.09	74.37	2.168
220.46	77.71	2.209	279.28	69.80	2.217
222.66	78.06	2.200	281.57	69.06	2.373
224.86	78.41	2.192			
226.60	79.14	2.172	Series 9 (metastable)		
228.77	79.15	1.166	248.12	69.27	2.378
230.93	79.71	2.157	250.50	69.03	2.379
233.08	80.03	2.151	252.87	68.90	2.377
235.23	80.37	2.145	255.25	68.72	2.376
238.11	81.06	1.601	257.62	68.62	2.375
240.19	81.36	2.129	259.99	68.66	2.372
242.31	82.01	2.120	262.36	68.62	2.370
244.42	82.50	2.113	264.73	68.61	2.368
246.53	82.86	2.017	269.09	68.52	2.367
248.63	83.32	2.100	269.50	68.47	2.451
250.72	83.91	2.092	271.92	68.40	2.391
252.80	84.48	2.084	274.30	68.29	2.389
254.88	85.11	2.075	276.69	68.23	2.388
256.95	85.84	2.067			
259.01	86.67	2.057			

increment ΔH to the temperature rise ΔT. The temperature indicated is the average of the initial and the final temperatures. Also shown is the approximate temperature rises. Figure 1 is the graphical representation of the heat capacity data. There are three regions of anomalously high heat capacity. As stated above, the transitions at 85°K and 266°K are very sluggish, the intermediate one being entirely normal. As a criterion for determining the heat capacity at these temperature range, it was assumed that the temperature variation after turning off the calorimeter heater follows

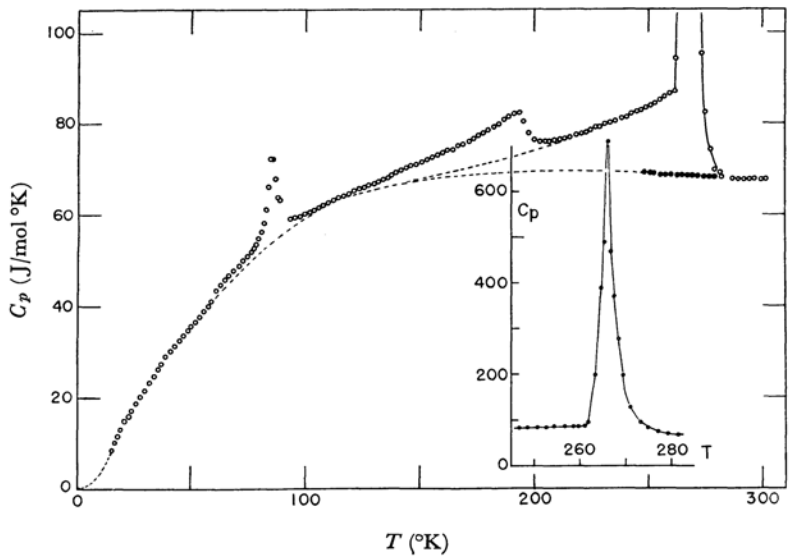

Fig. 1. Molar heat capacity *vs.* temperature of TlCN crystal.
(—○—○—○—; stable phase, —●—●—●—; the metastable cubic phase)

the exponential time dependence. That is

$$T(t) - T(\infty) = [T(0) - T(\infty)] \exp\left(-\frac{t}{\tau}\right),$$

where $T(t)$ is the temperature of the calorimeter at time t measured from the time when the heater is turned off, and τ, a time constant. Differentiation with t gives

$$\frac{dT}{dt} = -[T(0) - T(\infty)]\frac{1}{\tau}\exp\left(-\frac{t}{\tau}\right)$$
$$= -\frac{1}{\tau}[T(t) - T(\infty)].$$

Therefore, if we plot $T(t)$ against $dT(t)/dt$ extrapolation of the graph to $dT(t)/dt=0$ gives $T(\infty)$. In practice, the resistance $R(t)$ of the platinum thermometer was plotted rather than the temperature.

This method rests entirely on the assumption of the exponential time dependence of the temperature, which is not always the case. Therefore, it is applied solely, for the sake of convenience, to prohibitingly long equilibriation times.

TABLE 2. ENTHALPY AND ENTROPY CHANGES OF THE TRANSITIONS

T_{tr}(°K)	ΔS_{tr}(J/mol °K)	ΔH_{tr} (J/mol)
84.7	2.242	181.3
193.2	1.458	255.7
266.1	11.481	2945.5

The enthalpy and entropy changes of the phase transitions are summarized in Table 2 together with the temperature at which the heat capacity has the peaks. These values are of the corresponding changes associated with the excess heat capacity above the dotted curves in Fig. 1. The dotted curves are assumed to represent the vibrational part of the heat capacity. They are just the extrapolation of the heat capacity of the temperature ranges where anomalous effect seems to be absent. Their significance may be rather obscure in principle, but there are many cases in practice in which the entropy of the phase transition thus obtained can be rationalized in theoretical interpretations.

^{205}Tl NMR. The typical NMR absorption derivatives are shown in Fig. 2 for the room temperature and 210°K. The room temperature absorption is narrow and symmetric in its shape, while it becomes broad and slightly but significantly asymmetric at lower temperatures. Their second moment is shown in Fig. 3 as a function of temperature. The second moment of the asymmetric spectra was approximated by the sum of the lower field and higher halves which are separated by the zero of the absorption derivative. The second moment decreases steadily to about 180 °K and remains rather constant to the upper transition point where it decreases suddenly.

Figure 4 shows the field dependence of the second moment of the absorption at the room temperature

TABLE 3. THERMODYNAMIC PROPERTIES OF THALLOUS CYANIDE CRYSTAL*

T	$C_p°$	$S°$	$\frac{(H°-H°_0)}{T}$	$\frac{-(G°-H°_0)}{T}$	T	$C_p°$	$S°$	$\frac{(H°-H°_0)}{T}$	$\frac{-(G°-H°_0)}{T}$
5	(0.900)	(0.4351)	(0.2895)	(0.146)	140	69.274	85.565	42.396	43.169
10	(4.146)	(1.902)	(1.318)	(0.584)	150	71.433	90.423	44.263	46.160
15	9.456	4.573	3.121	1.452	160	73.580	95.106	46.028	49.078
20	14.016	7.539	5.343	2.196	170	75.663	99.628	47.706	51.922
25	18.012	11.510	7.456	4.054	180	78.375	104.086	49.334	54.692
30	21.945	15.144	9.556	5.588	190	81.768	108.35	50.949	57.401
35	25.773	18.816	11.594	7.222	193.2	Phase Transition			
40	29.342	22.493	13.602	8.891	200	76.397	112.46	52.405	60.056
45	32.606	26.140	15.527	10.613	210	76.232	116.17	53.526	62.644
50	35.673	29.735	17.392	12.343	220	77.655	119.75	54.589	65.158
60	43.099	36.778	20.949	15.829	230	79.433	123.21	55.630	67.578
70	48.501	43.855	24.527	19.328	240	81.412	126.63	56.664	69.966
80	55.083	50.695	27.865	22.830	250	83.705	130.00	57.697	72.299
84.7	Phase Transition				260	86.797	133.34	58.756	74.582
90	60.388	57.561	31.221	26.340	266.1	Phase Transition			
100	60.166	63.830	33.443	30.387	280	69.551	146.82	67.697	79.123
110	62.701	69.684	36.041	33.643	290	67.881	149.20	67.726	81.474
120	64.873	75.235	38.284	36.951	298.15	67.703	151.10	67.726	83.374
130	67.070	80.514	40.413	40.101	300	67.697	151.29	67.726	83.564

* The units are °K for temperature and J/mol°K for the other quantities.

and 210°K, the latter being a temperature where the second moment retains a rather constant value. The room temperature value is field-independent; this is what is expected for the dipolar and/or exchange broadening. In the low temperature phase, the second moment is definitely larger and depends linearly on the square of the static magnetic field. Similar type of behaviors was observed in Tl_2O_3,[4] Tl,[4] UF_6,[9] XeF_4,[10] $CFCl_2 \cdot CFCl_2$[11] and $CF_2Br \cdot CF_2Br$[11] and may be attributed to the anisotropic

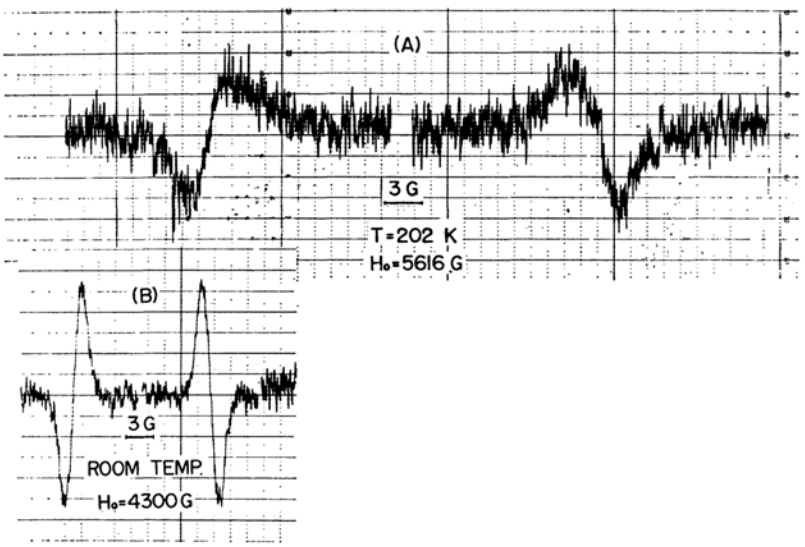

Fig. 2. ^{205}Tl NMR absorption derivatives of TlCN in the low temperature phase (A) and the cubic phase (B). In each case, the left half indicates sweeping up-field and the right half down-field.

9) R. Blinc, V. Marinkovic, E. Pirkmajer and I. Zupancic, *J. Chem. Phys.*, **38**, 2474 (1963).
10) R. Blinc, I. Zupancic, S. Maricic and Z. Vekseli, *ibid.*, **39**, 2109 (1963).
11) E. R. Andrew, D. T. Tunstall, *Proc. Phys. Soc.*, **81**, 986 (1963).

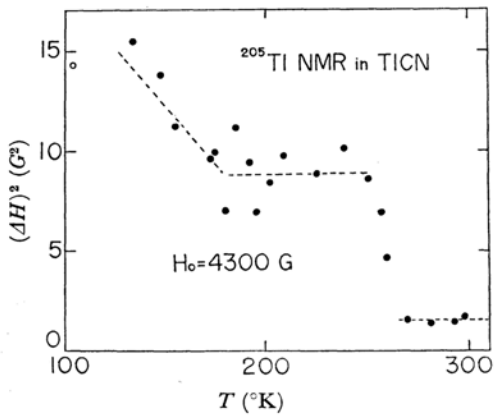

Fig. 3. Temperature dependence of apparent second moment of the ^{205}Tl NMR absorption in TlCN crystal.

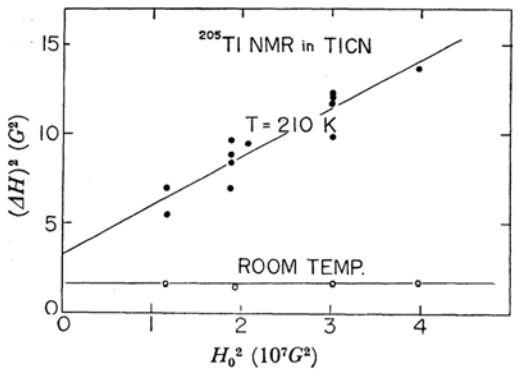

Fig. 4. Static field dependence of apparent second moment of the ^{205}Tl NMR absorption in TlCN crystal.

chemical shift.

Discussion

Phase Transitions. The total entropy associated with the three phase transitions is 15.2 J/mol°K. This value may be correlated with the possible eight directions of the cyanide ion on the four body diagonal directions in the cubic phase ($R\ln 8 = 17.2$ J/mol°K). The entropy change at the 266°K transition is approximately equal to $R\ln 4$, which implies that among the eight possible directions of the cyanide ion, two become energetically favored. This is the same situation as in the CsCN crystal. The CsCN crystal has a transition[3] at $T_{tr}=193.1$°K with $\Delta S_{tr}=15.7$ J/mol°K. Its low temperature phase has a distorted CsCl structure with one body diagonal axis elongated. If one assumes that TlCN has the same structure in the temperature region between the upper and the intermediate transitions, one can discuss the phase transition of the two salts comparatively. Among the possible molecular or ionic interactions leading to the transition, the dipole-dipole interaction between the CN^- ions is excluded on the symmetry ground. The next lower multipole is the quadrupole. The quadrupole-quadrupole interaction potential depends on the separation r as r^{-5}. The ratio of the lattice constant of TlCN to that of CsCN is equal to $a_{Tl}/a_{Cs}=3.993/4.25=0.9395$. If this value may be used also for the low temperature structures, its fifth power is expected to be approximately equal to the inverse ratio of the transition temperatures of the two salts. In fact, $(a_{Tl}/a_{Cs})^5=0.7320$ while $T_{Cs}/T_{Tl}=193.1/266.1=0.7257$. This excellent agreement may be rather fortuitous, since the change in the Madelung energy and the repulsive energy must be taken into account. However, before we are able to discuss these effects, it would be necessary to have more detailed structural informations. The scalar quadrupole moment of the CN^- ion was estimated to be $Q=0.7\times10^{-26}$cgs by equating kT_{tr} to the quadrupole-quadrupole interaction potential given by the expression[13]

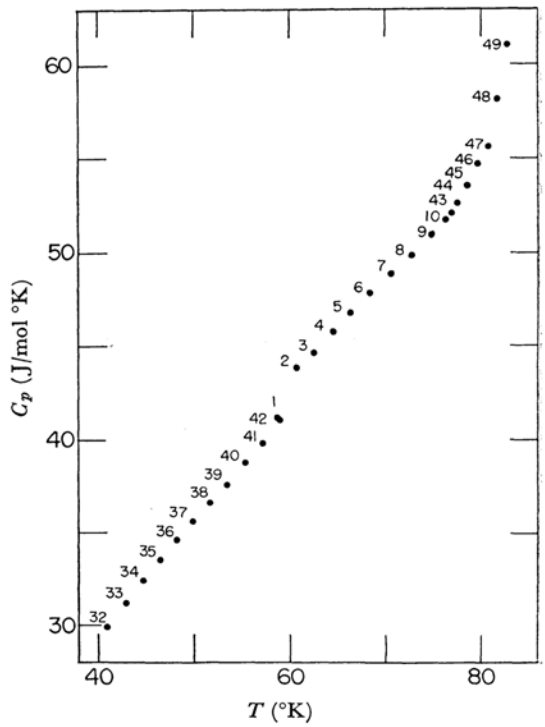

Fig. 5. The portion of the heat capacity diagram of TlCN crystal showing a small step-like anomaly. The numbers in the figure indicate the time order in which the measurements were performed.

12) J. O. Hirschfelder, C. F. Curtis, R. B. Bird, "Molecular Theory of Gases and Liquids," John Wiley & Sons, Inc., New York (1964), p. 27.

13) P. Goursot, E. F. Westrum, Jr., and J. Metzger, *Compt. Rend. Acad. Sci. Paris*, **266**, 590 (1968).

$$\Phi_{ab}^{(QQ)} = (3Q_aQ_b/16r^5)[1 - 5\cos^2\theta_a - 5\cos^2\theta_b - 15\cos^2\theta_a \cdot \cos^2\theta_b + \{2\sin\theta_a\sin\theta_b\cos(\phi_a - \phi_b) - 4\cos\theta_a\cos\theta_b\}^2],$$

where r is the intermolecular separation, θ's and ϕ's are polar and azimuthal angles measured from the intermolecular vector. Here, we used for the structural parameters their high temperature values. With regard to the other two phase transitions, no detailed interpretation seems to be possible at the present stage. In addition to these three anomalies, there is another which seems to be associated with the 85°K transition. The detailed diagram of the relevant portion of the heat capacity is shown in Fig. 5. It is not a peak but a steplike increase of the heat capacity. This type of anomaly is observed in many glass forming and other substances.[13,14] The interpretation of the detailed mechanism of this kind of transition remains for further investigations.

Hindered Rotation of the CN^- Ion. The heat capacities of the cubic phase in the stable and the metastable phases continue to each other smoothly as they should. The heat capacity value decreases with increasing temperature. This behavior is not feasible with the harmonic oscillator heat capacity. It is generally agreed that hindered rotation of molecules produces such an effect. There is wealth of literatures dealing with this phenomenon both from experimental and theoretical sides, the most recent and detailed treatment being due to Smith.[15] His investigation might be extended to apply to the present case.

The NMR Second Moment. From the NMR experiment we obtained a qualitatively interesting conclusion. The high temperature value of the second moment is comparable with the Van Vleck value for the dipolar broadening, while below the 266°K transition, it is definitely larger. The width might be due to the $I_1 \cdot I_2$ coupling through the electron and/or anisotropic chemical shift, since the lattice sum $\sum_{ij} 1/r_{ij}^6$ cannot change to this extent through the transition. Also the asymmetric shape of the spectrum suggests an anisotropic chemical shift. The slope of the line in Fig. 4 gives the anisotropy of the chemical shift, $\sigma^{\parallel} - \sigma^{\perp}$.[11] It is about 1000 ppm for the present case. If there are non-equivalent sites for the Tl ions, it may also contribute to the second moment with the similar H_0 dependence. But the asymmetric spectrum does not occur if the non-equivalent sites are same in number. Moreover, the spectrum would exhibit resolved structures if they were mere superpositions of a small number of the narrow spectra shifted from each other.*3

We can, therefore, conclude that the thallium chemical shift tensor changes on the phase transition, which in turn means that there are definite chemical bonds[16-20] among the ions which change on the phase transition. Thermodynamic consequences of such chemical bonds are still to be investigated.

Conclusion

Thallium cyanide crystal has three phase transitions below the room temperature. The uppermost one may be of the same nature as the one observed in cesium cyanide crystal. Interpretation of the other two transitions seems to be difficult at the present stage. The heat capacity of the cubic modification could be measured in the stable and the metastable temperature region and behaves as expected for a hindered rotator. ^{205}Tl NMR line widths in the low temperature phases are definitely larger than the dipolar width and may be attributed to the anisotropic chemical shift. This implies that not only the packing condition of the ions but also the electronic state changes on the phase transition to the extent to be observed in such an experiment.

The authors are grateful to Dr. Nobuo Nakamura, Osaka University, to whom they owe much in performing the NMR experiment. Also the financial support by the Toyo Rayon Co. is greatly acknowledged.

14) M. H. Brown and A. R. Taylor, Jr., private communication.

15) D. Smith, *J. Phys. Chem. Solids*, **29**, 525 (1968).

*3 The authors owe to Mr. G. Soda, Osaka University, for his pointing out these possibilities.

16) T. Kanda, *J. Phys. Soc. Japan*, **10**, 85 (1955).

17) K. Yoshida and T. Moriya, *ibid.*, **11**, 33 (1956).

18) J. Kondo and J. Yamashita, *J. Phys. Chem. Solids*, **20**, 243 (1959).

19) Y. Saito, *J. Phys. Soc. Japan*, **21**, 1072 (1966).

20) C. J. Jameson and H. S. Gutowsky, *J. Chem. Phys.*, **40**, 1714 (1964).